Hindawi Publishing Corporation
EURASIP Journal on Wireless Communications and Networking
Volume 2007, Article ID 73928, 6 pages
doi:10.1155/2007/73928

Research Article

60 GHz Indoor Propagation Studies for Wireless Communications Based on a Ray-Tracing Method

C.-P. Lim, M. Lee, R. J. Burkholder, J. L. Volakis, and R. J. Marhefka

ElectroScience Laboratory, Department of Electrical and Computer Engineering, Ohio State University, 1320 Kinnear Road, Columbus, OH 43212, USA

Received 28 April 2006; Revised 13 November 2006; Accepted 13 November 2006

Recommended by Chia-Chin Chong

This paper demonstrates a ray-tracing method for modeling indoor propagation channels at 60 GHz. A validation of the ray-tracing model with our in-house measurement is also presented. Based on the validated model, the multipath channel parameter such as root mean square (RMS) delay spread and the fading statistics at millimeter wave frequencies are easily extracted. As such, the proposed ray-tracing method can provide vital information pertaining to the fading condition in a site-specific indoor environment.

1. INTRODUCTION

Increasing demand of real-time high-speed applications calls for wireless local area network (LAN) operating in the 60 GHz band as part of the 4th generation (4G) system. The 60 GHz band has spiked great interest [1–7] because of its large bandwidth (7 GHz) allocated for future dense wireless local communications, particularly as relates to large wireless LAN bridges, and wireless high-quality video-conferencing. To establish such links, wireless systems which exploit time, frequency, and spatial multiplexing may be required. Design of these communication systems involves space-time coding, adaptive antennas, and rake reception which rely strongly on the characterization of the propagation channel. Previous work in channel characterizations at these millimeter (mm) wave frequencies have depended on measurements [2, 8–11]. However, measurements can be expensive (especially in the mm-wave band) as compared to electromagnetic (EM) modeling approaches. Since rigorous numerical methods are ruled out due to the very short wavelength at mm waves, we consider high-frequency asymptotic approaches such as ray-tracing (RT) method for modeling the channels. RT methods have the capability to solve electrically large problems relatively fast and, as such, they become an obvious candidate for the extraction of channel parameters. In this paper, we compare the channel parameters based on the RT model with in-house collected measurements, and measurements obtained from [8]. Subsequently, we provide results for the fading statistics of the received power in two typical indoor propagation channels, namely, within a room and in a hallway.

The paper is organized as follows. The next section presents the validation of the ray-tracing model using measurements in the 2-3 GHz band. Section 3 describes the EM modeling of the room and hallway, and the simulation setup. Extraction of the channel parameters and modeling of the fading statistics are presented in Section 4. Section 5 concludes the paper.

2. VALIDATION OF THE RAY-TRACING MODEL WITH MEASUREMENTS

The numerical electromagnetic code-basic scattering code (NEC-BSC) [12], which is based on 3-dimensional (3D) ray-tracing technique, utilizes the uniform asymptotic concepts formulated in terms of the uniform geometrical theory of diffraction (UTD) [13, 14]. As such, UTD is ideal for understanding the high-frequency response of signal in a complex environment whereby the basic structural features (that are crucial for accuracy) of that complex environment are necessary for modeling. In doing so, this allows for the use of ray optical techniques for obtaining the incident, reflected, and diffracted rays, contributed from these various basic structures. As a result, the reflected and diffraction fields are subsequently determined using the UTD solutions

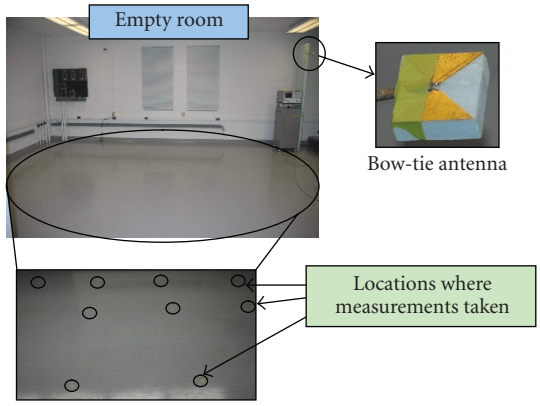

Figure 1: Photograph of the empty room where the measurements were conducted. The inset shows some of the measuring locations.

which consist of the individual rays that are summed with the geometrical optics in the far zone of the scatterer. As we know, the rays from a given scatterer tend to interact with other nearby objects, resulting into higher-order rays. As such, NEC-BSC was built to take care of all these high-order interactions, but not all high-order contributions are significant. Therefore, one can also choose to include only dominant contributions in NEC-BSC. Given all these, NEC-BSC is appropriate in this 60 GHz propagation study and it is employed to obtain power delay profiles (PDPs) for the indoor propagation channel. As a first step, we proceed to validate the ray-tracing model with measurements for the indoor propagation channel considered in this paper.

2.1. Measurement setup

The measurement setup consisted of a network analyzer (i.e., *Agilent* E8362B), a pair of 180° hybrid couplers, and a pair of identical bow-tie antennas (denoted as Antenna 1 and Antenna 2). The bow-tie antennas were designed to have a center frequency of 2.5 GHz, with fanning angle 45° and 1 GHz bandwidth sufficient for this measurement. An empty room was chosen (see Figure 1) whose dimensions are depicted in Figure 2. Specifically, the room is of length 7.72 m, width 5.84 m, and height 2.82 m. Antenna1, operating as a transmitter, was positioned at (0.94 m, 0.76 m) and at a height of 2.24 m. Antenna 2, serving as a receiver, was placed at 18 different locations inside the room (standing at the height of 1.12 m) for measurements. The detailed position of these 18 locations is depicted in Figure 2. For consistency, four measurements were taken at each of these locations and the average of these four measurements was used as the result. For each measurement, a total of 1601 frequency points (i.e., S_{21}) between 2 GHz and 3 GHz was used, resulting in a frequency step of 0.625 MHz. This frequency resolution implied a maximum excess delay of about 1600 ns and a temporal resolution of 1 ns (because of the 1 GHz bandwidth). We remark that a signal-to-noise ratio (SNR) of at least 20 dB was maintained throughout all measurements (via averaging during data sampling).

2.2. Simulations

For our simulations, the NEC-BSC was used. We computed the response at the same 1601 continuous wave (CW) tones evenly spaced between 2 GHz and 3 GHz as done with the measurements. For these calculations, the direct and reflected rays up to tenth order (from the walls, ceiling, and floor) were included. The walls, floor, and ceiling were characterized by relative dielectric constant $\epsilon_r = 4.22 - j0.02$ whereas the walls were of thickness 14.5 cm. The relative dielectric constant was taken from the detailed study of material characterization (based on measurements) documented in [15]. Both the transmitting and receiving antennas (i.e., Antenna1 and Antenna 2) were modeled in NEC-BSC as having a donut antenna pattern as shown in Figure 3. The figure shows the antenna pattern obtained from *Ansoft* HFSS simulation. These antennas (with the same dimensions) were built and used in our in-house measurements. As such, one would expect the antenna pattern in the measurements to be identical to the one obtained in HFSS simulation (refer to Figure 3). For the propagation study, the similar antenna pattern was employed in the NEC-BSC simulations. We remark that the simulation time of each location (based on NEC-BSC) was approximately 139 min using a 1.6 GHz central processing unit (CPU) machine.

2.3. Validation results

As is expected, one-to-one mapping of indoor propagation measurements to simulations is rarely achieved. As such, one can explore a stochastic way of validating the measurement and simulation data [16]. Specifically, we compared the time-domain multipath channel parameters such as mean excess delay and root mean square (RMS) delay spread [17]. These parameters are useful in describing the overall characteristics of the multipath profile and are essential in developing design guidelines for digital wireless communication systems. These channel parameters are easily extracted from the power delay profiles (PDPs). To obtain the PDP at a given receiver location, the 1601 CW tones are transformed to the time domain via an inverse fast Fourier transform (IFFT) procedure. Therefore, each of the 18 measuring locations (see Figure 2) is associated with a PDP and a set of multipath channel parameters. Of particular importance is the RMS delay spread (σ), which equals to the square root of the second moment of the PDP [17]. This is an indicator of the maximum data rate in the wireless channel and is also directly related to the performance degradation caused by intersymbol interference (ISI). Given the importance of RMS delay spread, we used this parameter for comparing the measured and calculated data. As 18 measuring locations were considered here, we built a cumulative distribution function (CDF) for the RMS delay spread values. Figure 4 shows the measured and simulated RMS delay spread CDFs. Clearly, there is a good agreement between

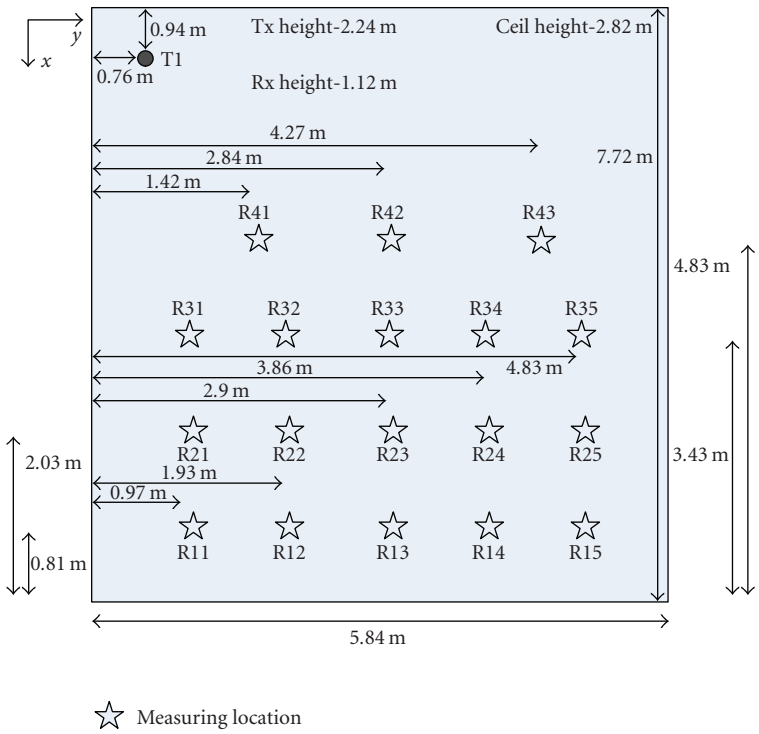

Figure 2: The positions of the 18 measuring locations and the transmitting location, all within the classroom of dimensions, length 7.72 m, width 5.84 m, and height 2.82 m.

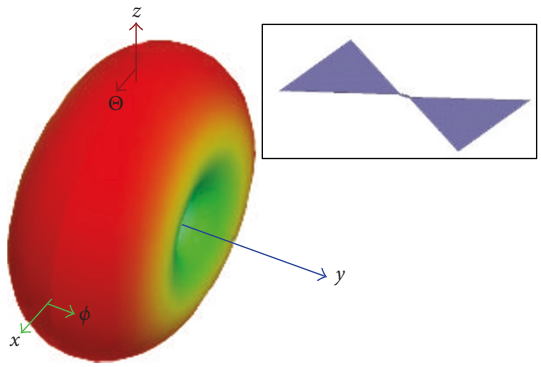

Figure 3: *Ansoft* HFSS simulation of the bow-tie antennas that were used for our in-house measurements; on the left is the antenna pattern and on the right is the bow-tie antenna HFSS model.

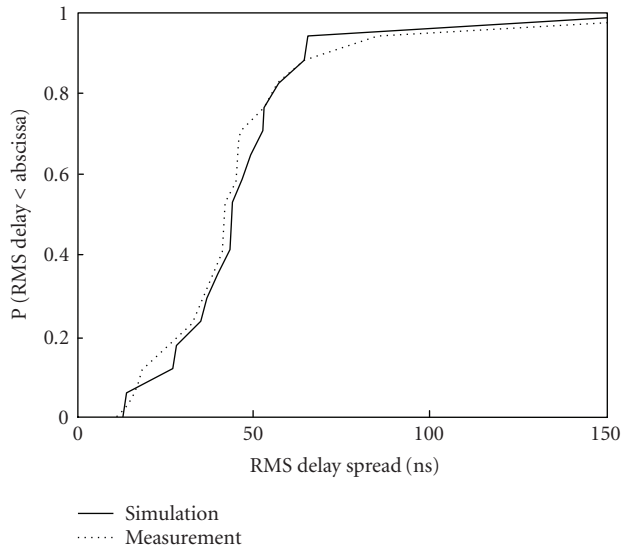

Figure 4: Comparison of measured and simulated RMS delay spread CDFs in the empty room; the solid line denotes the RMS delay spread obtained from our simulations; the dotted line represents the measured RMS delay spread.

measurements and simulations, indicating that the NEC-BSC can be employed for predicting the multipath channel parameters. As we know, NEC-BSC was formulated based on UTD concepts which are particularly ideal for high-frequency simulations. As such, one would anticipate when the ray-tracing modeling was appropriate at 2-3 GHz, it would also be valid at 60 GHz propagation modeling (since NEC-BSC employs high-frequency asymptotic approximations). Next, we proceed with a study at 60 GHz based on the NEC-BSC.

3. MODELING OF ROOM AND HALLWAY

For our 60 GHz propagation studies, of particular interest was the effect of wall configuration on the channel parameters and the fading statistics. Thus, we considered two

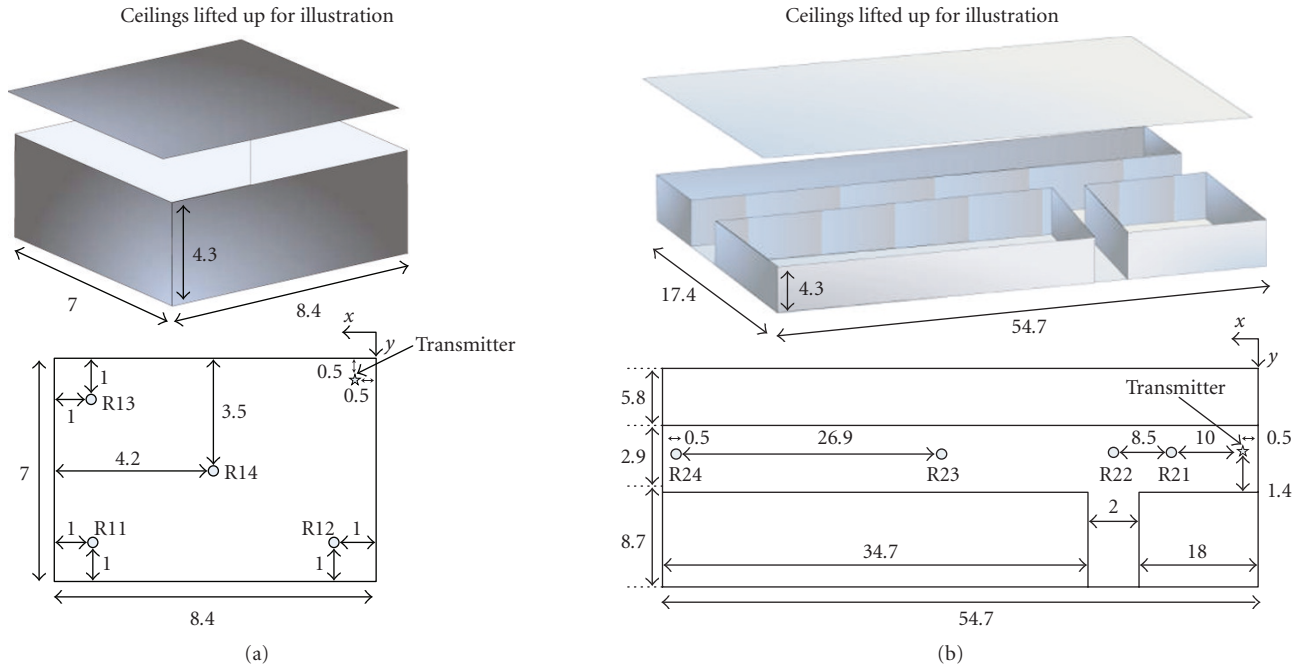

Figure 5: (a) 3D view of the room and its floorplan used for the 60 GHz simulations. (b) 3D view of the hallway and its floorplan. (All dimensions are in m.)

configurations: (1) a room and (2) a hallway. The dimensions of the room are depicted in Figure 5(a) and the dimensions of the hallway are depicted in Figure 5(b). The room has length 8.4 m, width 7.0 m, and height 4.3 m, whereas the hallway has length 54.7 m, width 2.9 m, and height 4.3 m. The walls, floor, and ceiling are 14.5 cm thick characterized by a relative dielectric $\epsilon_r = 4.22 - j0.02$. For propagation analysis, we chose a horn antenna as the transmitter with a theoretical half power beamwidths (HPBW) of 12° in azimuth and 9.5° in elevation. The receiving antennas were considered to have a donut antenna pattern (as shown in Figure 3). We remark that all receiver positions had a line-of-sight (LOS) path to the transmitter. Specifically, four receiving locations for both the room and hallway, namely, R11-R14 and R21-R24 were sampled (see Figure 5). At these locations, channel parameters and fading statistics were extracted as described in Section 4.

For the simulations, the NEC-BSC was set to analyze the propagation response using 1601 continuous wave (CW) tones evenly spaced between 59 GHz and 61 GHz, which results in a frequency sweep with 1.25 MHz steps. As a result, the frequency resolution had a maximum excess delay of about 166.66 ns and a temporal resolution of 500 ps (because of 2 GHz bandwidth). In the simulations, the direct and reflected rays up to tenth and seventh order from the walls, ceiling, and floor were included for the room and hallway, respectively. Here, our interest is the extraction of the multipath channel parameter (i.e., RMS delay spread). As such, the 1601 CW tones are transformed to time domain to obtain the channel response (i.e., PDP) at each receiver location. We note that the simulation times for each receiving location are approximately 67 min and 142 min for the room and hallway, respectively, using a 1.6 GHz CPU machine.

Table 1: RMS delay spread of room and hallway as shown in Figure 5.

Rx location	Room σ [ns]	Rx location	Hallway σ [ns]
R11-(7.4,6.0,1.6)	31.20	R21-(44.2,10.1,1.6)	58.15
R12-(1.0,6.0,1.6)	24.85	R22-(35.7,10.1,1.6)	65.32
R13-(7.4,1.0,1.6)	51.28	R23-(27.4,10.1,1.6)	51.88
R14-(4.2,3.5,1.6)	36.26	R24-(54.2,10.1,1.6)	57.44

4. CHANNEL PARAMETERS AND FADING MODEL

Next, we proceed to extract the multipath channel parameter (i.e., RMS delay spread σ) at 60 GHz. Table 1 shows the RMS delay spread at the various receiving locations for both the room and the hallway. When the receiving antenna is placed at different locations, the delay spread ranges from 24.85 ns to 51.28 ns for the room and from 51.88 ns to 65.32 nsec for the hallway. The simulated delay spreads are in agreement with the measurement results in [8]. In the case of [8], the delay spreads for indoor 60 GHz channels range from 15 ns to 45 ns for small rooms and between 30 ns and 70 ns for large indoor environments. This also implies that the ray-tracing method can be used to predict the multipath channel parameters at the mm-wave frequencies.

As is well known, indoor propagation involves interactions among furniture, walls, or other objects. Because of

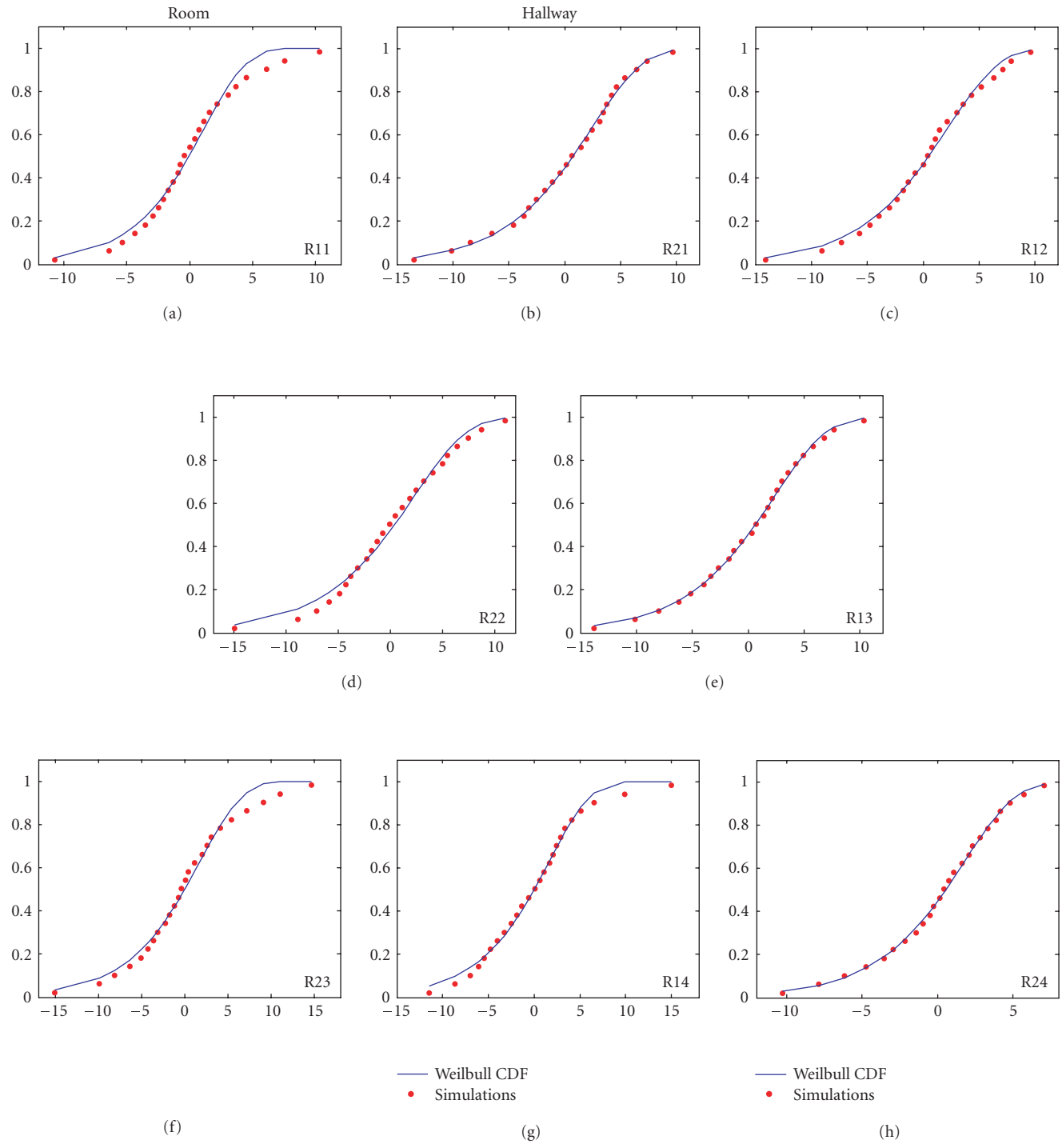

FIGURE 6: Cumulative distributive function (CDF) computed from the received power over mean power in Figure 5. The dots are CDF of the simulations of received power over mean power at R11-R14 and R21-24 and the depicted solid lines come from the best-fitted Weibull distribution.

these multipath, signals arrive at the receiver with different phases, causing fading. This fading can be obtained statistically from the PDPs by first developing a cumulative distributive function (CDF) based on the probability of receiving energies above a predetermined threshold level. Next, we look for the best-fit distribution for the observed CDF (by means of maximum likelihood estimation). In this analysis, we chose the Weibull distribution (which has also been used for ultra-wideband indoor propagation [18]) for fitting the data. The Weibull probability density function can

be written as

$$p(r) = \begin{cases} ba^{-b}r^{b-1}\exp\left(-\dfrac{r}{a}\right)^{b} & \text{for } 0 \le r \le \infty \\ 0 & \text{for } r < 0, \end{cases} \quad (1)$$

where a and b, respectively, are the scale and the shape parameters chosen to fit the simulations.

To check the fitting of the observed and estimated Weibull data, we performed a null hypothesis testing, H_0 : (observed data = fitted Weibull) versus the alternative hypothesis H_A : (observed data $\neq$ fitted Weibull) by using the Kolmogorov-Smirnov (KS) goodness-of-fit test. To ensure a good fit within a reasonable tolerance, the *significant level* was kept within 5%. In both the room and the hallway studies, it is clearly shown in Figure 6 that the CDFs at receiving locations (i.e., R11-R14 and R21-R24) have a good agreement with the Weibull distribution. We remark that the fitness of our simulations to other CDFs, specifically the Rayleigh CDF, can be found in [19, 20].

5. CONCLUSION

Based on the 3D ray-tracing method, we extracted statistical parameters (i.e, RMS delay spread) for indoor site-specific environments of different configurations. We found that the fading statistics of these indoor environments were characterized by a Weibull distribution. Accurate prediction of such statistics is vital in determining the channel capacity, and this has been shown in [21]. In conclusion, it has been demonstrated that the ray-tracing methods can be used for channel parameter extractions, particularly at 60 GHz band.

ACKNOWLEDGMENTS

The authors would like to thank the editor and the anonymous reviewers for their valuable comments and suggestions.

REFERENCES

[1] P. Smulders, "Exploiting the 60 GHz band for local wireless multimedia access: prospects and future directions," *IEEE Communications Magazine*, vol. 40, no. 1, pp. 140–147, 2002.

[2] H. Xu, V. Kukshya, and T. S. Rappaport, "Spatial and temporal characteristics of 60-GHZ indoor channels," *IEEE Journal on Selected Areas in Communications*, vol. 20, no. 3, pp. 620–630, 2002.

[3] T. Manabe, Y. Miura, and T. Ihara, "Effects of antenna directivity and polarization on indoor multipath propagation characteristics at 60 GHz," *IEEE Journal on Selected Areas in Communications*, vol. 14, no. 3, pp. 441–448, 1996.

[4] A. M. Hammoudeh and G. Allen, "Millimetric wavelengths radiowave propagation for line-of-sight indoor microcellular mobile communications," *IEEE Transactions on Vehicular Technology*, vol. 44, no. 3, pp. 449–460, 1995.

[5] S. Collonge, G. Zaharia, and G. El Zein, "Influence of the human activity on wide-band characteristics of the 60 GHz indoor radio channel," *IEEE Transactions on Wireless Communications*, vol. 3, no. 6, pp. 2396–2406, 2004.

[6] F. Giannetti, M. Luise, and R. Reggiannini, "Mobile and personal communications in the 60 GHz band: a survey," *Wireless Personal Communications*, vol. 10, no. 2, pp. 207–243, 1999.

[7] S. K. Yong and C. C. Chong, "An overview of multi-gigabit wireless through millimeter wave technology: potentials and technical challenges," to appear in *EURASIP Journal on Wireless Communications and Networking*.

[8] P. F. M. Smulders and L. M. Correia, "Characterisation of propagation in 60 GHz radio channels," *Electronics and Communication Engineering Journal*, vol. 9, no. 2, pp. 73–80, 1997.

[9] A. Hammoudeh, D. A. Scammell, and M. G. Sánchez, "Measurements and analysis of the indoor wideband millimeter wave wireless radio channel and frequency diversity characterization," *IEEE Transactions on Antennas and Propagation*, vol. 51, no. 10 II, pp. 2974–2986, 2003.

[10] N. Moraitis and P. Constantinou, "Indoor channel measurements and characterization at 60 GHz for wireless local area network applications," *IEEE Transactions on Antennas and Propagation*, vol. 52, no. 12, pp. 3180–3189, 2004.

[11] T. Zwick, T. J. Beukema, and H. Nam, "Wideband channel sounder with measurements and model for the 60 GHz indoor radio channel," *IEEE Transactions on Vehicular Technology*, vol. 54, no. 4, pp. 1266–1277, 2005.

[12] R. J. Marhefka, "Numerical electromagnetics code - basic scattering code (NEC-BSC Version 4.2), User's Manual," Tech. Rep. (Preliminary), ElectroScience Laboratory, The Ohio State University, Columbus, Ohio, USA, October 2000.

[13] R G. Kouyoumjian and P. H. Pathak, "A uniform geometrical theory of diffraction for an edge in a perfectly conducting surface," *Proceedings of the IEEE*, vol. 62, no. 11, pp. 1448–1461, 1974.

[14] P. H. Pathak, W. D. Burnside, and R. J. Marhefka, "A Uniform GTD analysis of the diffraction of electromagnetic waves by a smooth convex surface," *IEEE Transactions on Antennas and Propagation*, vol. 28, no. 5, pp. 631–642, 1980.

[15] A. H. Muqaibel, "Characterization of ultra wideband communication channels," Ph.D. dissertation, Virginia Polytechnic Institute and State University, Blacksburg, Va, USA, 2003.

[16] C.-C. Chong, Y.-E. Kim, S. K. Yong, and S.-S. Lee, "Statistical characterization of the UWB propagation channel in indoor residential environment," *Wireless Communications and Mobile Computing*, vol. 5, no. 5, pp. 503–512, 2005, special issue on Ultrawideband for Wireless Communications.

[17] T. S. Rappaport, *Wireless Communications: Principles and Practice*, Prentice-Hall, Upper Saddle River, NJ, USA, 1996.

[18] C.-C. Chong and S. K. Yong, "A generic statistical-based UWB channel model for high-rise apartments," *IEEE Transactions on Antennas and Propagation*, vol. 53, no. 8, part 1, pp. 2389–2399, 2005.

[19] R. J.-M. Cramer, R. A. Scholtz, and M. Z. Win, "Evaluation of an ultra-wide-band propagation channel," *IEEE Transactions on Antennas and Propagation*, vol. 50, no. 5, pp. 561–570, 2002.

[20] C.-P. Lim, R. J. Burkholder, J. L. Volakis, and R. J. Marhefka, "Propagation modeling of indoor wireless communications at 60GHz," in *Proceedings of IEEE AP-S International Symposium and USUC/URSI National Radio Science Meeting and AMEREM Meeting*, pp. 2149–2152, Albuquerque, NM, USA, July 2006.

[21] C.-P. Lim, J. L. Volakis, K. Sertel, R. W. Kindt, and A. Anastasopoulos, "Indoor propagation models based on rigorous methods for site-specific multipath environments," *IEEE Transactions on Antennas and Propagation*, vol. 54, no. 6, pp. 1718–1725, 2006.